International Journal of Modern Physics E
Vol. 27, No. 1 (2018) 1850001 (14 pages)

DOI: 10.1142/S0218301318500015

Theoretical estimates of the width of light-meson states in the SO(4) (2+1)-flavor limit

Tochtli Yépez-Martínez* and Osvaldo Civitarese†

Departamento de Física,
Universidad Nacional de La Plata,
C.C.67 (1900), La Plata, Argentina
**yepez@fisica.unlp.edu.ar*
†osvaldo.civitarese@fisica.unlp.edu.ar

Peter Otto Hess

Instituto de Ciencias Nucleares,
Universidad Nacional Autónoma de México,
Ciudad Universitaria, Circuito Exterior S/N,
A.P. 70-543, 04510 México, D.F., México
hess@nucleares.unam.mx

Received 14 August 2017
Revised 29 November 2017
Accepted 1 December 2017
Published 9 January 2018

The low-energy sector of the mesonic spectrum exhibits some features which may be understood in terms of the SO(4) symmetry contained in the QCD-Hamiltonian written in the Coulomb Gauge. In our previous work, we have shown that this is indeed the case when the Instantaneous Color-Charge Interaction (ICCI) is treated by means of nonperturbative many-body techniques. Continuing along this line of description, in this work we calculate the width of meson states belonging to the low portion of the spectrum ($E < 1$ GeV). In spite of the rather simple structure of the Hamiltonian used to calculate the spectra of pseudoscalar and vector mesons, the results for the width of these states follow the pattern of the data.

Keywords: Meson states; nonperturbative QCD; RPA approach; widths.

PACS Number(s): 12.38.−t, 12.40.Yx, 21.60.Fw, 14.40.−n

1. Introduction

The QCD is at low energy a highly nonperturbative theory. Continuous efforts are undertaken to treat QCD nonperturbatively, a regime where the *Lattice Gauge Theory* (LGT)[1] is considered to be the only one which can do this from a fundamental basis. In the description of low-lying hadron states[2,3] and of high-lying meson states[4] some progress has been made. In LGT, the rotational symmetry is broken

and it requires some effort to recover the continuum limit. The complete spectrum cannot be obtained and, in addition, the numerical effort is considerable.

There are other attempts, like the use of the *Dyson–Schwinger equations*,[5] which succeeded, for example, in explaining the chiral symmetry breaking.[6] However, also these attempts suffer from some drawbacks, like truncation schemes applied in the functional approach which need to be controlled and tested.

Therefore, it is worth investigating alternative methods, which require much less numerical effort and maintain spherical symmetry. For example, in Ref. 7, the QCD-Hamiltonian at low energy was diagonalized in a continuum basis in momentum space, using for the Coulomb interaction a static, confining potential. In Ref. 8, a general calculation of baryon states was performed, allowing high-spin couplings of the quarks. But also there, the numerical calculation required a lot of time (months), whose origin is in the continuum momentum basis, which makes it difficult to localize a state.

Before trying to perform a realistic treatment, it is useful to start from a simplified model. Such a method was applied in Ref. 9, were the kinetic energy term of the QCD-Hamiltonian was diagonalized within the harmonic oscillator basis. The oscillator basis consists of already localized states with the disadvantage of not being relativistic, which requires larger matrices. In fact, a practical treatment always boils down to looking for the optimal basis. The model, including a static confining potential, was presented in Ref. 10, for a QCD motivated Hamiltonian for light quarks. It was shown that a description of low-lying physical meson states can be given in terms of the eigenstates of the Casimir operator of the SO(4) group, since a sector of the QCD-Hamiltonian possesses such a symmetry. In the same work,[10] it was shown that the pion-like meson state is an eigenstate of the Casimir operator, of the singlet SO(4) representation, with zero energy.

In Ref. 11, the chiral and flavor symmetries, present in the above-mentioned SO(4) limit of the QCD-Hamiltonian discussed in Ref. 10, were broken and a (2+1)-flavor description for light and strange quarks was used. The effective Hamiltonian was diagonalized in a basis of quark–antiquark pairs by applying the *Random Phase Approximation* (RPA) method. The motivation of this contribution is to test a simple procedure for the calculation of the decay width within the SO(4) model, for meson-like states. This will help in establishing, furthermore, the limitations of the SO(4) model space for the description of physical mesons.

The method is introduced in Ref. 12, which is based on the interaction of a physical state with its background states. We calculate the width of meson-like states in the basis of effective degrees of freedom contained in the SO(4) model of Refs. 10 and 11. Although the model is rather simple, it has the advantage of a relatively small number of effective degrees of freedom, a feature which facilitates the identification of physical states by their quark contents. Our hope is that the manner to determine the decay widths can be applied to more involved models, until we reach the full QCD at low energy.

The paper is organized as follows. In Sec. 2, we briefly describe the essentials of the QCD-SO(4) model, introduce its RPA treatment and the formalism used to calculate the width of the states. In Sec. 3, we present and discuss the results of the calculations. Finally, we summarize our conclusions in Sec. 4.

2. Formalism

2.1. *SO*(4) *model and its RPA solutions*

In Ref. 10, the SO(4) Hamiltonian was proposed, using a similar expression as obtained in Ref. 13, i.e., it reflects the same structure of a realistic QCD-Hamiltonian.

Using

$$\begin{aligned}
\hat{A} &= \sum_m C^\dagger_{2m} C_{1m}, \\
\hat{B} &= \sum_m C^\dagger_{2m} C_{1-m}, \\
\hat{C} &= \hat{A}^\dagger, \\
\hat{D} &= \hat{B}^\dagger, \\
\hat{E} &= \sum_{\sigma,m} \frac{(-1)^\sigma}{2} C^\dagger_{\sigma m} C_{\sigma m} \\
\hat{F} &= \sum_{\sigma,m} \frac{(-1)^\sigma}{2} C^\dagger_{\sigma m} C_{\sigma -m},
\end{aligned} \tag{1}$$

where the $C^\dagger_{\sigma m}$ and $C_{\sigma m}$ are creation and annihilation operators, respectively, of particles in the substate (m) of the upper 2 or lower 1 level of the SO(4) model space, and with the association

$$\begin{aligned}
&\hat{A} = \hat{J}_+, \quad \hat{C} = \hat{J}_-, \quad \hat{E} = \hat{J}_0, \\
&\hat{B} = \hat{V}_+, \quad \hat{D} = \hat{V}_-, \quad \hat{F} = \hat{V}_0,
\end{aligned} \tag{2}$$

the Hamiltonian acquires the structure

$$\begin{aligned}
H_{\mathrm{RPA}}[\mathrm{SO}(4)] = {} & (\epsilon_f C^\dagger_{2m,f} C_{2m,f} - \epsilon_{f'} C^\dagger_{1m,f'} C_{1m,f'}) - a_7 \hat{V}_0 + a_2 \hat{V}_0^2 + a_3 \hat{J}_0^2 \\
& + a_6 \hat{V}_0 \hat{J}_0 + \frac{a_1}{2} (\hat{J}_+ \hat{J}_- + \hat{V}_+ \hat{V}_-) \\
& + \frac{a_5}{2} (\hat{J}_+ \hat{V}_- + \hat{V}_- \hat{J}_+ + h.c.) + b((\hat{J}_+ + \hat{V}_+)(\hat{J}_+ + \hat{V}_+) + h.c.).
\end{aligned} \tag{3}$$

This Hamiltonian is ordered into contributions H_{ij}, where i refers to the number of creation and j to the number of annihilation operators appearing in each term.

This general Hamiltonian for quarks and antiquarks has one-body terms $H_{11} + H_{20} + H_{02}$ and two-body terms $H_{22} + H_{31} + H_{13} + H_{40} + H_{04}$. In Ref. 11, we have

implemented the RPA method and found meson-like solutions for a Hamiltonian of the following form:

$$H_{\mathrm{RPA}} = H_{11} + H_{22} + H_{40} + H_{04}, \tag{4}$$

where each term of the Hamiltonian is expressed in terms of the SO(4)-group generators obtained for a system of particles and holes described in Ref. 10.

Four sets of parameters are used for the coefficients (a_i, b) of the Hamiltonian of Eq. (3) leading to four different scenarios for the low-energy meson-like spectrum.[10] The sets of parameters and the corresponding solutions are denoted by *Set*-1,2,3 and 4. The calculated spectrum, for each set of parameters, has 16 eigenvalues which are associated to physical meson-states, according to their dominant flavor content and energy, as we shall discuss later on. The values are listed in Ref. 10. These energies and wave functions are used to calculate the widths of the states, in the manner described in the next section The procedure is taken from Ref. 12

2.2. *The width of the states*

The Hamiltonian is written

$$H = H_0 + V, \tag{5}$$

where H_0 is the Hamiltonian of Eq. (3) mapped onto the RPA basis

$$H_0 = \sum_n E_n^{\mathrm{RPA}} \gamma_n^\dagger \gamma_n \tag{6}$$

with $n = 1, \ldots 16$. The operator $\gamma_n^\dagger$ (γ_n) creates (annihilates) the nth one-phonon state. The interaction term (V), describes the interactions not included in the RPA treatment.[11] To calculate the width of a state $|a\rangle = \gamma_a^\dagger |\tilde{0}\rangle$, we assume that the basis can be separated in a set of reference states $\{|a\rangle\}$ and a background $\{|\alpha\rangle\}$ with N elements, such that[12]

$$\begin{aligned} H_0|a\rangle &= E_a|a\rangle, \\ H_0|\alpha\rangle &= E_\alpha|\alpha\rangle, \\ \langle a|V|a\rangle &= 0, \\ \langle \alpha_j|V|\alpha_{j'}\rangle &= V_{\alpha_j,\alpha_{j'}} = 0 \quad \forall\, j, j', \\ \langle a|V|\alpha_j\rangle &= V_{a,\alpha_j} = V_{\alpha_j,a} = \text{real}, \end{aligned} \tag{7}$$

leading to the Hamiltonian-matrix

$$H = \begin{pmatrix} E_a & V_{a,\alpha_1} & V_{a,\alpha_2} & V_{a,\alpha_3} & \cdots & V_{a,\alpha_N} \\ V_{a,\alpha_1} & E_{\alpha_1} & 0 & 0 & \cdots & 0 \\ V_{a,\alpha_2} & 0 & E_{\alpha_2} & 0 & \cdots & 0 \\ . & . & . & . & . & \\ V_{a,\alpha_N} & 0 & 0 & 0 & \cdots & E_{\alpha_N} \end{pmatrix}. \tag{8}$$

Any eigenstate of the Hamiltonian of Eq. (5) can be written as

$$|E\rangle = c_a(E)|a\rangle + \sum_j c_{\alpha_j}(E)|\alpha_j\rangle. \tag{9}$$

So that

$$H|E\rangle = c_a(E)(H_0+V)|a\rangle + \sum_j c_{\alpha_j}(E)(H_0+V)|\alpha_j\rangle = E|E\rangle, \tag{10}$$

where

$$\begin{aligned} \langle a|H|E\rangle &= Ec_a(E) = c_a(E)E_a + \sum_j c_{\alpha_j}(E)V_{a,\alpha_j}, \\ \langle \alpha_j|H|E\rangle &= Ec_{\alpha_j}(E) = c_a(E)V_{a,\alpha_j} + c_{\alpha_j}(E)E_{\alpha_j}. \end{aligned} \tag{11}$$

The above equations and the normalization condition $\langle E \mid E\rangle = 1$ lead to the amplitudes

$$\begin{aligned} c_{\alpha_j}(E) &= -c_a(E)\frac{V_{a,\alpha_j}}{(E_{\alpha_j}-E)}, \\ (c_a(E))^2 &= \left(1+\sum_j \frac{\left(V_{a,\alpha_j}\right)^2}{(E_{\alpha_j}-E)^2}\right)^{-1}. \end{aligned} \tag{12}$$

Then, the mean value of the energy, $\bar{E}$, and the width, Γ, of the state with $E \approx E_a$ are given by the expressions[14]

$$\begin{aligned} \bar{E} &= E_a(c_a(E))^2 + \sum_j E_{\alpha_j}(c_{\alpha_j}(E))^2, \\ \Gamma &= 2\sigma = 2\left((E_a-\bar{E})^2(c_a(E))^2 + \sum_j (E_{\alpha_j}-\bar{E})^2(c_{\alpha_j}(E))^2\right)^{\frac{1}{2}}. \end{aligned} \tag{13}$$

Note, that the main ingredients for the determination of Γ and V_{a,a_j} are the expansion coefficients $c_a(E)$ and c_{α_j}, the first for the physical reference state and the second for the background states, both expanded in the basis. With their knowledge and the help of the first line in Eq. (11), the matrix elements V_{a,α_j} are determined. These V_{a,α_j} are in general not the same but similar within a set, which justifies the use of the approximation of a constant coupling V (see further below). To obtain the value of V an average over all value V_{a,α_j} has to be applied. Note, that the V is not adjusted to the width of a particular state but rather is a consequence of the expansion coefficients evaluated in the basis of SO(4).

3. Numerical Analysis of the Solutions: Energy and Widths of Meson-Like States

The low-energy scalar-meson states have large widths.[15] This is the case of the state tentatively identified as $f_0(500)$ (or σ) with a width of about 400–700 MeV. The

existence and the structure of this scalar-meson state has been rather controversial since it could be interpreted as a four-quark state or as a two-meson molecule.[16] In Ref. 13, we were able to identify scalar-mesons as solutions of a nonperturbative approach based on the use of many-body methods. However, scalar-meson states are beyond the reach of the minimal SO(4)-model developed in Refs. 10 and 11 since angular or radial excitations are needed to get quark–antiquarks meson-like states of positive parity. For pseudoscalar mesons up to 1 GeV, the data indicate that they have narrower widths while broader widths are reported for vector mesons. That is the case of the ρ-meson. In Table 1 we list the values taken from Ref. 15.

The width of the $\eta'(957)$ state is about 0.02% of the mass of the state. Because of this rather small value it will be considered as an isolated state. For the rest of the states, their widths vary between $\approx 1\%$ and 20% of their masses and they will be calculated using the formalism presented in the previous section. In the following, we shall perform a case-by-case analysis of the results obtained with each set of parameters of the Hamiltonian of Eq. (3). They are listed in Table 2. The meaning of this parametrization, their values and the effects of it upon the meson spectrum have been discussed in detail in Refs. 10 and 11.

We have solved the RPA-eigenvalue problem and classified the eigenvectors by inspecting their flavor content in order to establishe a correspondence between the RPA spectrum and physical states. The results of such a procedure are given in Table 3.

Due to the SO(4) symmetry of the Hamiltonian the ρ- and ω-like states appear as a mixture, as well as the kaon (K, K^*)-like states.[10] The breaking of this degeneracy is beyond the SO(4) scheme since it requires the inclusion of radial and orbital excitations. As seen from the results listed in Table 3 for the set 1 there was only one possible state, at 716.44 MeV, that resembles the flavor structure of the η and η' states. We have assumed that these states are degenerate. The ϕ-like states obtained for set-1, show a small energy difference of about 22 MeV. For the calculations we will consider that the state at 1011 MeV represents the physical meson $\phi(1020)$

Table 1. Observed values of the widths Γ of pseudoscalar and vector mesons. The values are given in units of [MeV] and they have been taken from Ref. 15.

Width\State	η	ρ	ω	K^*	η'	ϕ
Γ	1.3	147.8	8.5	50.8	0.2	4.3

Table 2. Parameters of the Hamiltonian of Eq. (3). The values are given in units of [MeV].

Set	a_1	a_2	a_3	a_5	a_6	a_7	b
1	100	50	200	−300	100	−150	45.00
2	100	100	200	0	50	−50	58.12
3	100	−100	200	0	100	−150	54.37
4	100	150	200	0	0	0	54.37

Table 3. RPA energies, in units of MeV, for the eigenvectors associated to physical states[15] accordingly to the structure of their wave functions. The values in parenthesis indicate the degeneracy of each state. The sum of the degeneracies of each set equals the number of eigenvalues of the RPA basis.

State	Set 1	Set 2	Set 3	Set 4
π	184.81 (1)	164.49 (1)	187.27 (1)	201.37 (1)
$\rho\ \omega$	579.10 (3)	590.31 (3)	364.98 (3)	622.56 (3)
η	716.44 (1)	670.06 (1)	735.12 (3)	741.59 (1)
η'		965.95 (1)	895.17 (1)	1042.88 (1)
$K\ K^*$ (low)	780.00 (4)	780.00 (4)	402.11 (1)	780.00 (4)
$K\ K^*$ (high)	827.55 (3)	863.27 (3)	780.00 (4)	930.00 (3)
ϕ	1011.00 (1) 1033 (3)	1086.41 (3)	1039.89 (3)	1087.43 (3)

state, and that the other ϕ-like-states belong to the background. The set-3 gives in the kaon-like sector of the spectrum one state at low energy (402.11 MeV) as compared with the results obtained with the other sets of parameters. This state resembles more likely the pseudoscalar kaon and it will not be considered for the width analysis. For the rest of the kaon-like states of *Set*-1,2,3,4, the formalism presented in the previous section will be implemented in order to determine their widths.

Following the use of the formalism of the previous section, we have calculated the energy centroids and the average interaction for each of the states. The average value of the interaction which produces the broadening of the states is shown in Table 5.

As said before, the calculation of the width depends upon the choice of physical and background states and the nature of each state is being determined by the composition of its wave function in terms of quark–antiquark pairs. To give an idea about the structure of the RPA eigenvalues in Figs. 1–4, we show the collectivity of the states obtained with the different sets of parameters. The corresponding amplitudes are represented by the number of pairs which contributed to each meson-like state.

Table 4. Calculated width Γ Eq. (13) of the states, in units of MeV. The values have been obtained as described in the text. The result quoted for Set 3, sector K, K^*(high) corresponds to the vector state since Set 3 distinguish the K state from the K^* state.

State	Set 1	Set 2	Set 3	Set 4
$\rho\ \omega$	147.84	147.46	147.14	147.23
η	1.2	1.32	1.30	1.32
$K\ K^*$ (low)	50.82	50.90		50.63
$K\ K^*$ (high)	50.74	50.81	50.99	50.99
ϕ	4.30	4.32	4.29	4.32

Table 5. Energy centroids $\bar{E}$ and averaged interaction energy V, in units of MeV, for each of the sets of parameters considered in the calculations.

	Set 1		Set 2		Set 3		Set 4	
State	$\bar{E}$	V	$\bar{E}$	V	$\bar{E}$	V	$\bar{E}$	V
$\rho\ \omega$	598.91	45.15	610.43	45.5	367.87	34.5	645.69	50.00
η	716.44	0.20	670.06	0.20	735.12	0.29	741.59	0.20
$K\ K^*$ (low)	787.03	14.05	783.11	12.80			781.36	12.60
$K\ K^*$(high)	825.80	12.35	862.75	12.10	779.61	12.30	930.36	12.10
ϕ	1011.04	0.65	1086.39	1.02	1039.88	0.96	1087.40	1.02

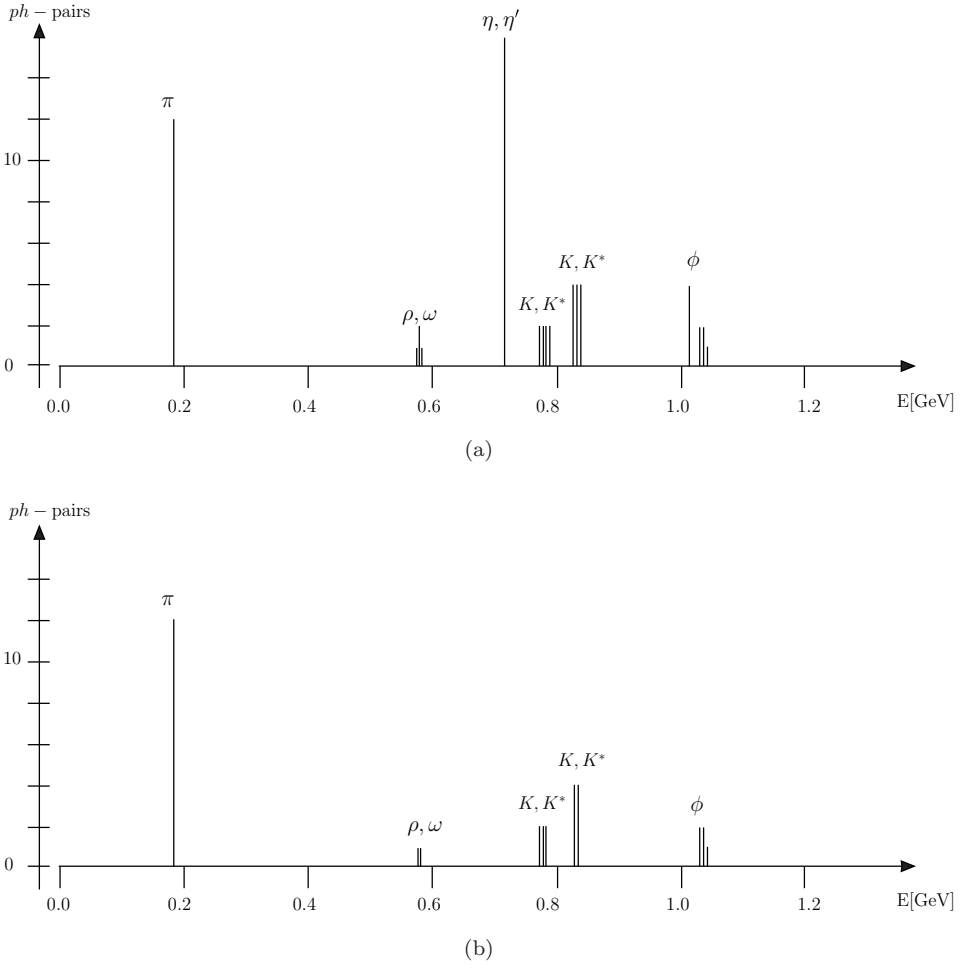

Fig. 1. Set-1: Structure of the RPA-eigenvalues, in terms of the number of particle (quark)–hole(antiquark) pairs. The upper inset (a) shows the complete RPA spectrum. In the lower inset (b) the composition of the background-states is shown.

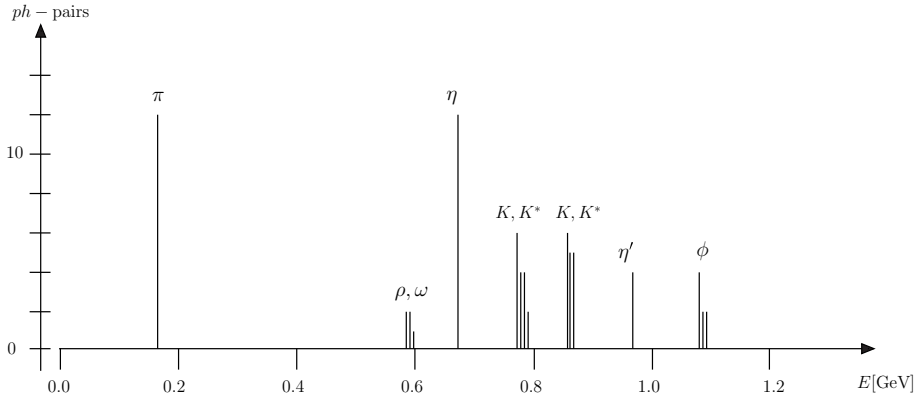

(a)

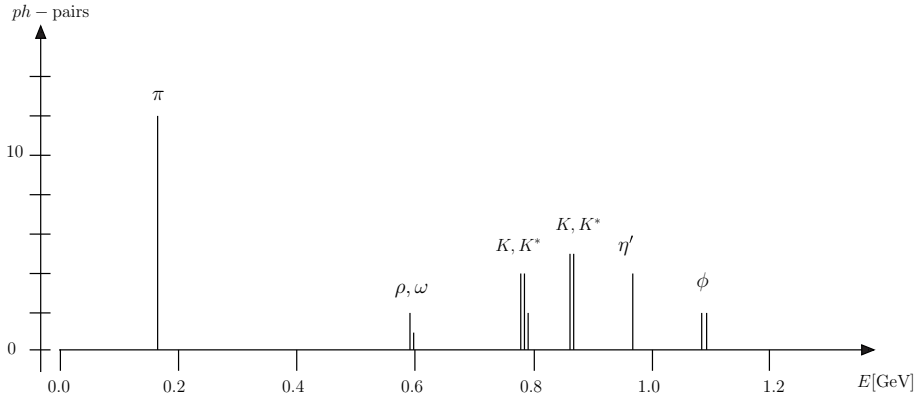

(b)

Fig. 2. Same as Fig. 1, for the Set-2 of parameters.

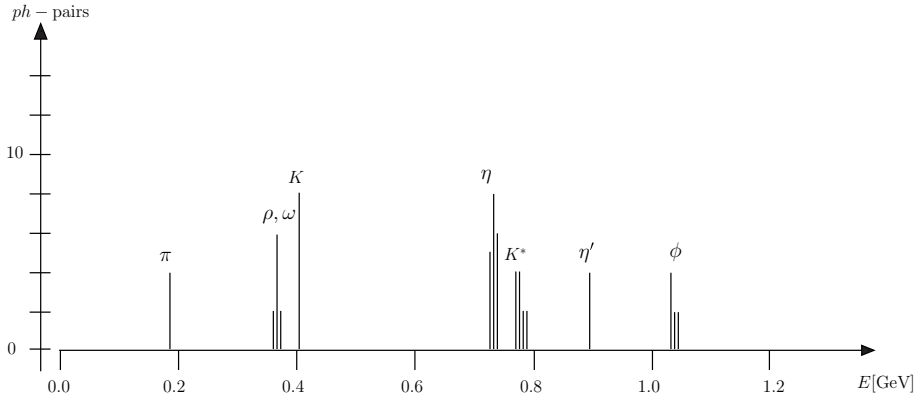

(a)

Fig. 3. Same as Fig. 1, for the Set-3 of parameters.

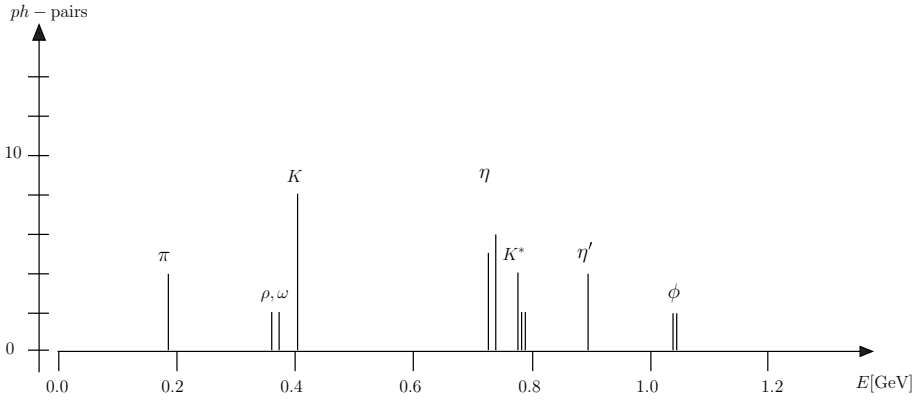

(b)

Fig. 3. (*Continued*)

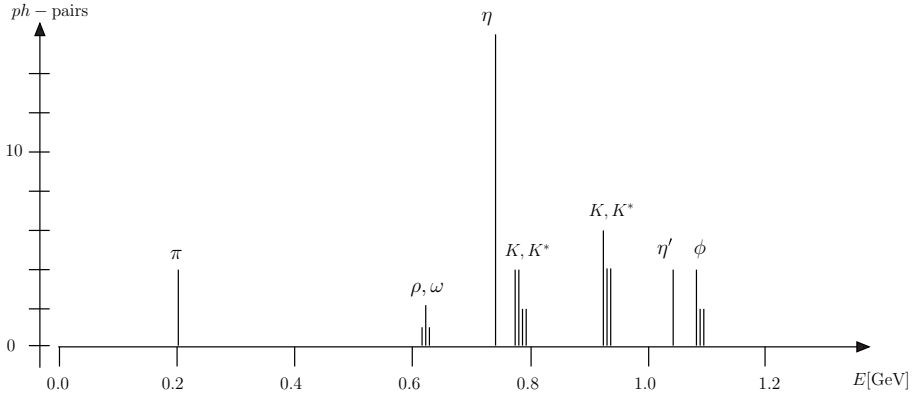

(a)

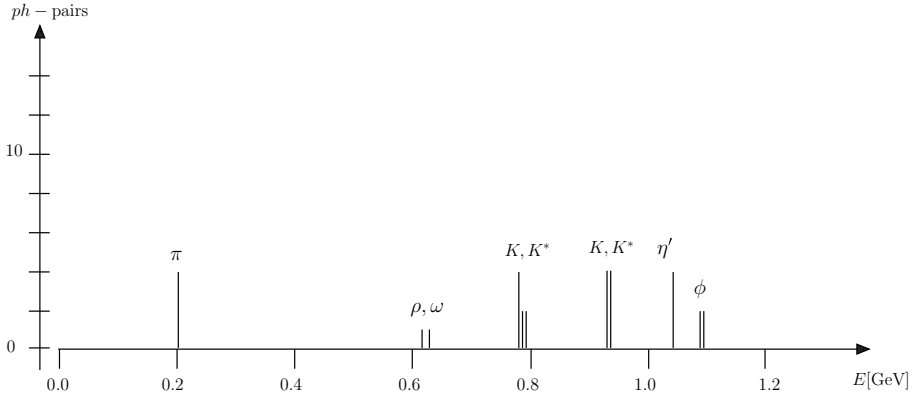

(b)

Fig. 4. Same as Fig. 1, for the Set-4 of parameters.

For example, the amplitudes for the case of the ρ, ω-like states are listed for the four different sets in the Tables 6, 8, 10, 12 and Tables 7, 9, 11, 13. These are the the coefficients appearing in Eqs. (9) and (11).

In all the scenarios shown before, the kaon sector of the SO(4) spectrum gives two different energies for the kaon-like states. The energy-gap between them is smaller, for Sets-1, 2 and 4, than the observed energy separation. The analysis of Set-3 indicates two well separated kaon-like states. Their energies correspond to 402 MeV and 780 MeV, which are comparable to the physical pseudoscalar

Table 6. List of the coefficients $c_a(E) = c_a$ and $c_{\alpha_j}(E) = c_{\alpha_j}(\Omega)$ for the meson–like states of Set-1 and their corresponding degeneration (Ω).

Ref. state	c_a	$c_\pi(1)$	$c_\rho(2)$	$c_{K(\text{low})}(3)$	$c_{K(\text{high})}(2)$	$c_\phi(3)$
ρ, ω	0.4932	−0.0514	−0.5772	0.1371	0.1061	0.0536
η, η'	0.9999	−0.0003	−0.0014	0.0031	0.0018	0.0006
$K, K^*(\text{low})$	0.5554	−0.0127	−0.0355	−0.4253	0.2673	0.0332
$K, K^*(\text{high})$	0.7366	−0.0137	−0.0338	−0.1336	−0.4438	0.0492
ϕ	0.9986	−0.0007	−0.0015	−0.0028	−0.0035	0.0294

Table 7. $|c_a(E)|^2$ and $|c_{\alpha_j}(E)|^2$ values for the meson-like states of Set-1 and their corresponding degeneration (Ω).

Ref. state	$\lvert c_a\rvert^2$	$\lvert c_\pi\rvert^2(1)$	$\lvert c_\rho\rvert^2(2)$	$\lvert c_{K(\text{low})}\rvert^2(3)$	$\lvert c_{K(\text{high})}\rvert^2(2)$	$\lvert c_\phi\rvert^2(3)$
ρ, ω	0.2432	0.0026	0.3332	0.0188	0.0113	0.0029
η, η'	≈1	≈0	≈0	≈0	≈0	≈0
$K, K^*(\text{low})$	0.3085	0.0002	0.0013	0.1809	0.0714	0.0011
$K, K^*(\text{high})$	0.5426	0.0002	0.0011	0.0179	0.1970	0.0024
ϕ	0.9973	≈0	≈0	≈0	≈0	0.0009

Table 8. List of the coefficients $c_a(E) = c_a$ and $c_{\alpha_j}(E) = c_{\alpha_j}(\Omega)$ for the meson-like states of Set-2 and their corresponding degeneration (Ω).

Ref. state	c_a	$c_\pi(1)$	$c_\rho(2)$	$c_{K(\text{low})}(3)$	$c_{K(\text{high})}(2)$	$c_{\eta'}$	$c_\phi(3)$
ρ, ω	0.4878	−0.0478	−0.5780	0.1467	0.0946	0.0658	0.0484
η	0.9999	−0.0003	−0.0025	0.0018	0.0010	0.0006	0.0004
$K, K^*(\text{low})$	0.6486	−0.0130	−0.0396	−0.4233	0.1304	0.0499	0.0289
$K, K^*(\text{high})$	0.7170	−0.0121	−0.0297	−0.0853	−0.4731	0.1028	0.0423
ϕ	0.7029	−0.0007	−0.0014	−0.0023	−0.0032	0.0060	0.5028

Table 9. $|c_a(E)|^2$ and $|c_{\alpha_j}(E)|^2$ values for the meson-like states of Set-2 and their corresponding degeneration (Ω).

Ref. state	$\lvert c_a\rvert^2$	$\lvert c_\pi\rvert^2(1)$	$\lvert c_\rho\rvert^2(2)$	$\lvert c_{K(\text{low})}\rvert^2(3)$	$\lvert c_{K(\text{high})}\rvert^2(2)$	$\lvert c_{\eta'}\rvert^2$	$\lvert c_\phi\rvert^2(2)$
ρ, ω	0.2379	0.0023	0.3341	0.0215	0.0089	0.0043	0.0023
η	≈1	≈0	≈0	≈0	≈0	≈0	≈0
$K, K^*(\text{low})$	0.4208	0.0002	0.0016	0.1792	0.0170	0.0025	0.0008
$K, K^*(\text{high})$	0.5142	0.0001	0.0009	0.0073	0.2239	0.0106	0.0018
ϕ	0.4941	≈0	≈0	≈0	≈0	≈0	0.2529

Table 10. List of the coefficients $c_a(E) = c_a$ and $c_{\alpha_j}(E) = c_{\alpha_j}(\Omega)$ for the meson-like states of Set-3 and their corresponding degeneration (Ω).

Ref. state	c_a	$c_\pi(1)$	$c_\rho(2)$	$c_{K(\text{low})}(1)$	$c_\eta(2)$	$c_{K(\text{high})}(3)$	$c_{\eta'}(1)$	$c_\phi(2)$
ρ, ω	0.7238	−0.2122	0.4157	0.2569	0.0580	0.0525	0.0423	0.0339
η	0.7095	−0.0003	−0.0005	−0.0006	0.4982	0.0045	0.0012	0.0006
K^*	0.7131	−0.0142	−0.0200	−0.0218	−0.1296	−0.3849	0.0949	0.0369
ϕ	0.7033	−0.0007	−0.0010	−0.0011	−0.0022	−0.0026	−0.0047	0.5026

Table 11. $|c_a(E)|^2$ and $|c_{\alpha_j}(E)|^2$ values for the meson-like states of Set-3 and their corresponding degeneration (Ω).

Ref. state	$\lvert c_a\rvert^2$	$\lvert c_\pi\rvert^2(1)$	$\lvert c_\rho\rvert^2(2)$	$\lvert c_{K(\text{low})}\rvert^2(1)$	$\lvert c_\eta\rvert^2(2)$	$\lvert c_{K(\text{high})}\rvert^2(3)$	$\lvert c_{\eta'}\rvert^2(1)$	$\lvert c_\phi\rvert^2(2)$
ρ, ω	0.5240	0.0451	0.1729	0.0660	0.0034	0.0028	0.0018	0.0011
η	0.5035	≈0	≈0	≈0	0.2482	≈0	≈0	≈0
K^*	0.5086	0.0002	0.0004	0.0005	0.0168	0.1481	0.0090	0.0013
ϕ	0.4947	≈0	≈0	≈0	≈0	≈0	≈0	0.2526

Table 12. List of the coefficients $c_a(E) = c_a$ and $c_{\alpha_j}(E) = c_{\alpha_j}(\Omega)$ for the meson-like states of Set-4 and their corresponding degeneration (Ω).

Ref. state	c_a	$c_\pi(1)$	$c_\rho(2)$	$c_{K(\text{low})}(3)$	$c_{K(\text{high})}(2)$	$c_{\eta'}(1)$	$c_\phi(2)$
ρ, ω	0.4413	−0.0480	−0.5824	0.1845	0.0818	0.0577	0.0516
η	0.9999	−0.0003	−0.0016	0.0052	0.0010	0.0006	0.0005
$K, K^*(\text{low})$	0.6834	−0.0143	−0.0483	−0.4147	0.0666	0.0355	0.0300
$K, K^*(\text{high})$	0.6995	−0.0113	−0.0260	−0.0506	−0.4931	0.0884	0.0603
ϕ	0.7004	−0.0008	−0.0015	−0.0023	−0.0045	−0.0165	0.5045

Table 13. $|c_a(E)|^2$ and $|c_{\alpha_j}(E)|^2$ values for the meson-like states of Set-4 and their corresponding degeneration (Ω).

Ref. state	$\lvert c_a\rvert^2$	$\lvert c_\pi\rvert^2(1)$	$\lvert c_\rho\rvert^2(2)$	$\lvert c_{K(\text{low})}\rvert^2(3)$	$\lvert c_{K(\text{high})}\rvert^2(2)$	$\lvert c_{\eta'}\rvert^2(1)$	$\lvert c_\phi\rvert^2(2)$
ρ, ω	0.1948	0.0023	0.3393	0.0341	0.0067	0.0033	0.0026
η	≈1	≈0	≈0	≈0	≈0	≈0	≈0
$K, K^*(\text{low})$	0.4671	0.0002	0.0023	0.1720	0.0044	0.0013	0.0009
$K, K^*(\text{high})$	0.4894	0.0001	0.0007	0.0025	0.2431	0.0078	0.0036
ϕ	0.4906	≈0	≈0	≈0	≈0	0.0003	0.2545

K(495) and vector K*(892) kaon-states. This scenario reproduces approximately the experimental energy-difference, thus within the SO(4) scheme the kaon-like state to be associated with the physical pseudoscalar kaon is the one obtained with the Set-3. Even though the energy of low-lying kaon-like states obtained with Sets-1, 2 and 4 are not in good correspondence with the observed energy of the pseudoscalar K-state, and a clear identification of both the pseudoscalar and vector kaon-like states is not feasible, we have used both kaon-like sectors $(K, K^*(\text{low}))$ and $(K, K^*(\text{high}))$ to estimate the width of the states. In such scenarios, it will not be possible to describe the transition $\phi \to 2K$, except for the results obtained

with Set-3, and this shows a clear limitation of spectrum obtained with the SO(4) model.

By comparing the data of Table 1 with the calculated values listed in Table 4, we see that the agreement is quite remarkable considering the rather simple structure of the Hamiltonian, which is the SO(4) version of the QCD-Hamiltonian in the Coulomb Gauge. In all cases, the order of magnitude is correct and the sensitivity of the calculations with respect to the structure of the light-meson states is very strong since it correlates one by one with the physical states. The calculated values are indeed quite good, particularly in view of the huge variation of the data, which for the η-meson assigns a width of the order of 1.3 MeV and in the other extreme assigns much larger value (147.8 MeV) to the ρ-meson.

The features shown by the numerical results are indeed supported by the analytical solutions of the model, e.g. the ones obtained by using an average interaction proportional to the average energy spacing and degeneracies of the states. From the grouping of states around a given reference state, shown in Figs. 1–4., it is possible to extract an average interaction and take the analytic limit of the model, e.g., one state merged in the background. The results of such a calculation yield values of the interaction quite similar to those of Table 5.[a]

4. Summary

In this work, we have extended the study of our previous publications concerning the treatment of the QCD-Hamiltonian in the Coulomb Gauge. We have taken the dominant sector of it as to be represented by the generators of the SO(4) symmetry and parametrized the structure of the Hamiltonian in terms of the Casimir operators of the group, in order to calculate the spectrum of light-meson states. The Hamiltonian was diagonalized by applying the RPA method, which yields eigenvalues whose eigenvectors could be associated to physical states after analyzing their composition in terms of quark and antiquark pairs.[10,11] In order to test these wave functions, we have calculated the energy-width of each state by letting them interact with a background of less-collective or non-collective states. We have found that the calculated values do agree with the data, for the four sets of parameters considered in the calculations. Though the spectrum depends smoothly upon the parameters of the Hamiltonian, the calculation of the width of the states is parameter-free once the spectrum of physical and background states is properly defined. The transitions between the reference state and the background were calculated by using an average interaction for each type of meson-like states, in order to extract information about the structure of the states. For this, we have analyzed the amplitudes obtained by diagonalization in the sub-spaces, and found that the identification of the states which we have performed, by looking at their particle–hole content, is

[a]In the limit of an equidistant array of energies, the relationship between the width Γ, the energy spacing D and the average matrix element V is given by $\Gamma = 2\pi V^2/D$.[12]

physically sound. The relatively good agreement obtained by applying this method in the limited scenario of the SO(4) model, seems to indicate that it may also provide a suitable framework to calculate the decay width of meson-like states in more realistic situations, that is by dealing with more realistic model spaces and Hamiltonians. Work is in progress concerning the use of the present method in the case of the Hamiltonian of Ref. 13, where the RPA treatment of the QCD-Hamiltonian in the Coulomb Gauge was not restricted to the SO(4) limit.

Acknowledgments

One of the authors (T.Y-M) thanks the National Research Council of Argentina (CONICET) for a post-doctoral scholarship. (O.C.) is a member of the scientific career of the CONICET. (P.O.H) acknowledges financial help from DGAPA-PAPIIT (IN100315) and from CONACYT (Mexico, grant 251817). This work has been supported financially by the CONICET (PIP-282) and by the ANPCYT of Argentina.

References

1. W. Bietenholz, *Int. J. Mod. Phys. E* **25** (2016) 1642008.
2. Z. Fodor and C. Hoelbling, *Rev. Mod. Phys.* **84** (2012) 449.
3. FLAG Working Group, (S. Aoki *et al*). *Eur. Phys. J. C* **74** (2014) 2890.
4. J. J. Dudek *et al., Phys. Rev. D* **83** (2011) 111502(R).
5. G. Eichmann, H. Sanchis-Alepuz, R. Williams, R. Alkofer and C. S. Fischer, *Prog. Part. Nucl. Phys.* **91** (2016) 1.
6. A. Bashir *et al., Comm. Theor. Phys.* **58** (2012) 79.
7. F. J. Llanes-Estrada and S. R. Cotanch, *Nucl. Phys. A* **697** (2002) 303; *Phys. Rev. Lett.* **84** (2000) 1102.
8. P. Bicudo. M. Cardoso, F. J. Llanes-Estrada and T. Van Cauteren, *Phys. Rev. D* **94** (2016) 054006.
9. T. Yépez-Martńez, P. O. Hess, A. P. Szczepaniak and O. Civitarese, *Phys. Rev. C* **81** (2010) 045204.
10. T. Yepez-Martinez, O. Civitarese and P. O. Hess, *Int. J. Mod. Phys. E* **25** (2016) 1650067.
11. T. Yepez-Martinez, O. Civitarese and P. O. Hess, *Int. J. Mod. Phys. E* **26** (2017) 1750012.
12. A. Bohr and B. R. Mottelson, *Nuclear Structure V.I* (World Scientific, Singapore, 1999).
13. D. A. Amor-Quiroz, T. Yépez-Martńez, P. Hess, O. Civitarese and A. Weber, arXiv:1704.01947.
14. D. Bes and O. Civitarese, *Nucl. Phys. A* **741** (2004) 60.
15. Particle Data Group, (C. Patrignani *et al.*) *Chin. Phys. C* **40** (2016) 100001.
16. M. Albaladejo and J. A. Oller, *Phys. Rev. D* **86** (2012) 034003.